



EUROPEAN
COMMISSION

Community research



Long-term Performance of Engineered Barrier Systems PEBS

THM Model validation modelling of selected WP2 experiments

Inverse Modelling of the FEBEX in situ test using iTOUGH2

DELIVERABLE-N°: D3.3-1

Contract (grant agreement) number: FP7 249681

Author(s):

Uli Kuhlman¹, Irina Gaus²

¹ TK Consult, Switzerland, ² Nagra, Switzerland

Date of issue of this report: 27/03/2014

Start date of project: 01/03/10

Duration : 48 Months

Project co-funded by the European Commission under the Seventh Euratom Framework Programme for Nuclear Research & Training Activities (2007-2011)		
Dissemination Level		
PU	Public	PU
RE	Restricted to a group specified by the partners of the [acronym] project	
CO	Confidential, only for partners of the [acronym] project	

PEBS



Arbeitsbericht NAB 14-20

**Inverse modelling of the
FEBEX in situ test using iTOUGH2
(Deliverable D3.3-1 of the
PEBS Project)**

February 2014

U. Kuhlmann, I. Gaus

Nationale Genossenschaft
für die Lagerung
radioaktiver Abfälle

Hardstrasse 73
CH-5430 Wettingen
Telefon 056-437 11 11

www.nagra.ch

Arbeitsbericht NAB 14-20

**Inverse modelling of the
FEBEX in situ test using iTOUGH2
(Deliverable D3.3-1 of the
PEBS Project)**

February 2014

U. Kuhlmann, I. Gaus

KEYWORDS

Engineered Barrier Systems (EBS), bentonite, inverse modelling iTOUGH, thermo-hydraulic modelling

**Nationale Genossenschaft
für die Lagerung
radioaktiver Abfälle**

Hardstrasse 73
CH-5430 Wettingen
Telefon 056-437 11 11

www.nagra.ch

Nagra Working Reports concern work in progress that may have had limited review. They are intended to provide rapid dissemination of information. The viewpoints presented and conclusions reached are those of the author(s) and do not necessarily represent those of Nagra.

"Copyright © 2014 by Nagra, Wettingen (Switzerland) / All rights reserved.

All parts of this work are protected by copyright. Any utilisation outwith the remit of the copyright law is unlawful and liable to prosecution. This applies in particular to translations, storage and processing in electronic systems and programs, microfilms, reproductions, etc."

Table of contents

Table of contents	I
List of tables	II
List of figures	II
1 Introduction	1
1.1 Background	1
1.2 Objectives	1
1.3 Organisation of the report	1
2 The FEBEX <i>in situ</i> test	3
2.1 General description	3
2.2 Timeline of the experiment	4
2.3 Observation data	5
3 Conceptual model	9
3.1 Modelling approach	9
3.2 Model geometry	9
3.3 Initial and boundary conditions (BC)	11
3.3.1 Hydraulic conditions	11
3.3.2 Thermal boundary conditions	12
3.4 Inverse Framework	12
4 Model parameters, Prior Information	15
5 Results	17
5.1 Simulations results	17
5.2 Residual analysis	20
5.2.1 Pressure	20
5.2.2 Temperature	21
5.2.3 Relative humidity	21
5.3 Estimated parameters	26
6 Summary and Conclusion	29
7 References	31
8 Appendix	33

List of tables

Tab. 2.1:	Timeline of the FEBEX in-situ test	5
Tab. 3.1:	Chain of models with components involved (in addition to open drift entrance and host rock)	10
Tab. 4.1:	Hydraulic and thermal properties of the granite at the Grimsel Test Site (Finsterle & Pruess, 1995; Alonso et al., 2005; ENRESA, 2006)	15
Tab. 4.2:	Hydraulic and thermal properties of the FEBEX buffer (Alonso et al.; 2005, ENRESA, 2006)	16
Tab. 4.3:	Two-phase (modified) van Genuchten parameter models in iTOUGH2 (Finsterle, 2012) used for all materials	16
Tab. 5.1:	Hydraulic, thermal and two-phase properties of the different materials resulting from inverse modelling of the FEBEX-in-situ experiment (in brackets the computed standard deviations)	27

List of figures

Fig. 2.1:	FEBEX drift in a northern zone of the Grimsel Test Site (adapted from ENRESA, 2006)	3
Fig. 2.2:	Layout of the FEBEX in situ test, with locations of the sensed sections (from ENRESA, 2006)	4
Fig. 2.3:	Longitudinal section through test area with location of sensors TSD1-xx (cross-section D1) and TSD2-xx (cross-section D2)	6
Fig. 2.4:	Instrumented section F1 through test area with location of sensors (QBF12-xx, TBF12-xx)	7
Fig. 2.5:	Instrumented section F2 through test area with location of sensors (QBF23-xx, QBF24-xx, TBF23-xx, TBF24-xx)	7
Fig. 2.6:	Instrumented section D1 and D2 through test area with location of sensors TSD1-08, TSD1-10, TSD2-12 and TSD2-13	8
Fig. 3.1:	Axisymmetric mesh incl. lamprophyre and fracture FR-2, model dimensions, details and boundary conditions (mesh as used in the heating phase I)	10
Fig. 3.2:	<i>left</i> : 3D visualization of the axisymmetric mesh (Lamprophyre/fracture not shown) <i>right</i> : radial mesh refinements at the interfaces between heater, buffer, and EDZ	11
Fig. 3.3:	Hydraulic situation in the vicinity of the FEBEX drift, natural flow gradient (from ENRESA, 2006)	11
Fig. 3.4:	Log of temperature and power in Heater #1 during the first 762 days (from ENRESA, 2006)	12
Fig. 3.5:	Inverse framework: Iteratively running a series of models in order to minimize the objective function	13

Fig. 5.1:	Pressure distribution after excavation (phase INI), isothermal hydration (ISO), operational phase I (HT1).....	18
Fig. 5.2:	Temperature distribution after heating phase 1 (HT1), cooling down of Heater#1 (phase DMC), and after second heating phase with only heater#2 operating (HT2)	19
Fig. 5.3:	Distribution of water saturation after isothermal hydration (phase ISO), heating phase 1 (HT1), dismantling of Heater#1 (DMH), heating phase 2 (HT2)	20
Fig. 5.4:	Cross section F1 - comparison of measured and computed pressure in granite	22
Fig. 5.5:	Cross section F2 - comparison of measured and computed pressure in granite	22
Fig. 5.6:	Cross section F2 - comparison of measured and computed temperature in granite	23
Fig. 5.7:	Cross section F2 - comparison of measured and computed temperature in granite	23
Fig. 5.8:	Cross sections D1 (left) and D2 (right) - comparison of measured and computed temperature in bentonite (locations see Fig. 2.3)	24
Fig. 5.9:	Cross sections G (left) and I (right) - comparison of measured and computed temperature in bentonite (locations see Fig. 2.3)	24
Fig. 5.10:	Cross sections F1 and F2 - comparison of measured and computed relative humidity in bentonite	25
Fig. 5.11:	Cross section H - comparison of measured and computed relative humidity in bentonite	25
Fig. 5.12:	Retention curves of Grimsel granite and FEBEX bentonite (adapted from ENRESA, 2006)	27
Fig. 5.13:	Thermal conductivity and error range of FEBEX bentonite estimated by inverse modelling (adapted from ENRESA, 2006)	28
Fig. A.1:	Temperature – Section B1, B2.....	33
Fig. A.2:	Temperature – Section K1, K2	33

1 Introduction

1.1 Background

This study is part of the project PEBS (= Long-term Performance of Engineered Barrier Systems) which was initiated with main aim “to bridge the gap between the improved scientific understanding of THM-C processes and the actual needs of PA to specify EBS related safety function indicators. This comprises the development of systematic validation procedures for THM-C models, allowing for a quantitative evaluation of their predictive capabilities through a traceable prediction evaluation process.” (PEBS, 2010).

The present project is motivated by task WP3.3 and tests if TH inverse approaches can be applied for interpreting long term THM experiments and by task WP 3.5 which is dealing with extrapolation of findings from the (relatively short term) experiments and modelling efforts of the PEBS. In this context, the long term evolution of heat as emitted by nuclear waste and its impact on the saturation behaviour of the engineered barrier system (EBS) is being simulated.

1.2 Objectives

Usually, a coupled thermo-hydro-mechanical approach (THM) has to be applied due to swelling of the buffer material in order to predict the hydration process after closure of a repository. The high computational demand of THM-models, however, often prevents long term prediction runs and the evaluation of parameter sensitivities required by the performance assessment of the repository concept. In this regard, an attempt will be made to apply the computationally more efficient TH-code TOUGH2 (Pruess et al., 2011), thus, neglecting the mentioned mechanical processes. However, in order to ensure predictive reliability the involved model parameters have to be derived prior to extrapolation. In this context, inverse modelling of an appropriate in-situ experiment, the FEBEX in situ (ENRESA, 2006), is proposed in order to estimate consisting parameters and to demonstrate the applicability of the approach. The general question will be addressed if one can find model parameters based on the TH approach that are able to fit long term THM data reliably.

1.3 Organisation of the report

A brief overview of the FEBEX in situ heating test is given below in Chapter 2. Then, the conceptual model including its numerical approach, the implemented geometry and boundary conditions is described in Chapter 3 together with details on the inverse modelling framework. Best guess starting parameters found in documents and publications on the experiment are specified in Chapter 4. Simulation results, comparisons of model and measurements as well as estimated model parameters are described in Chapter 5. A summary and some concluding remarks can be found in the final Chapter 6.

2 The FEBEX *in situ* test

2.1 General description

The full-scale engineered barriers experiment (FEBEX) in crystalline host rock “in situ” test is an almost 1:1 physical model of the Spanish reference disposal concept. The “in situ” test was installed in a drift excavated in the northern zone of the underground laboratory at the Grimsel Test Site. (GTS), (s. Fig. 2.1).

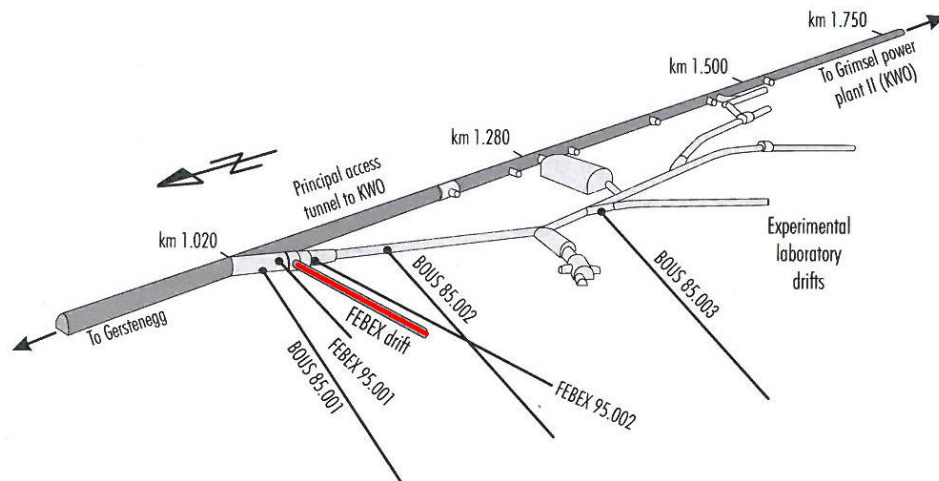


Fig. 2.1: FEBEX drift in a northern zone of the Grimsel Test Site (adapted from ENRESA, 2006)

Fig. 2.2 represents the test schematically as initially built. The physical components of the test consist of five basic units: the drift, the heating system, the clay barrier, the instrumentation, and the monitoring and control system. The drift has a length of 70.4 m and a diameter of 2.28 m, and is excavated in a granite rock mass. In the last 17.4 m of the drift, the basic elements of the test were installed and the section was sealed with a concrete plug (ENRESA, 2006).

Two major hydraulic features intersecting the drift are associated with the lamprophyre dyke that intersects near Heater#1 and fracture FR-2 that intersect at $x \sim 54\text{m}$ (Fig. 2.2). It is expected that these features are some orders of magnitude more permeable than the background granite.

The main elements of the heating system are two heaters located within a steel liner installed concentrically with the drift. The heaters simulate the canisters at real size. The clay barrier is formed from blocks of highly compacted bentonite. After 5 years of operation partial dismantling has consisted of extracting one heater and corresponding clay barrier and of sealing the remaining section of the test with a new concrete plug.

The instrumentation includes the sensors installed in the heaters, clay barrier, and surrounding rock. The variables measured are: temperature, humidity, stress, total pressure, displacement, and water pressure.

In addition, the generation and transport of gas is being measured. A detailed description of set-up, performance, modelling and interpretation of the experiment is given in ENRESA (2006).

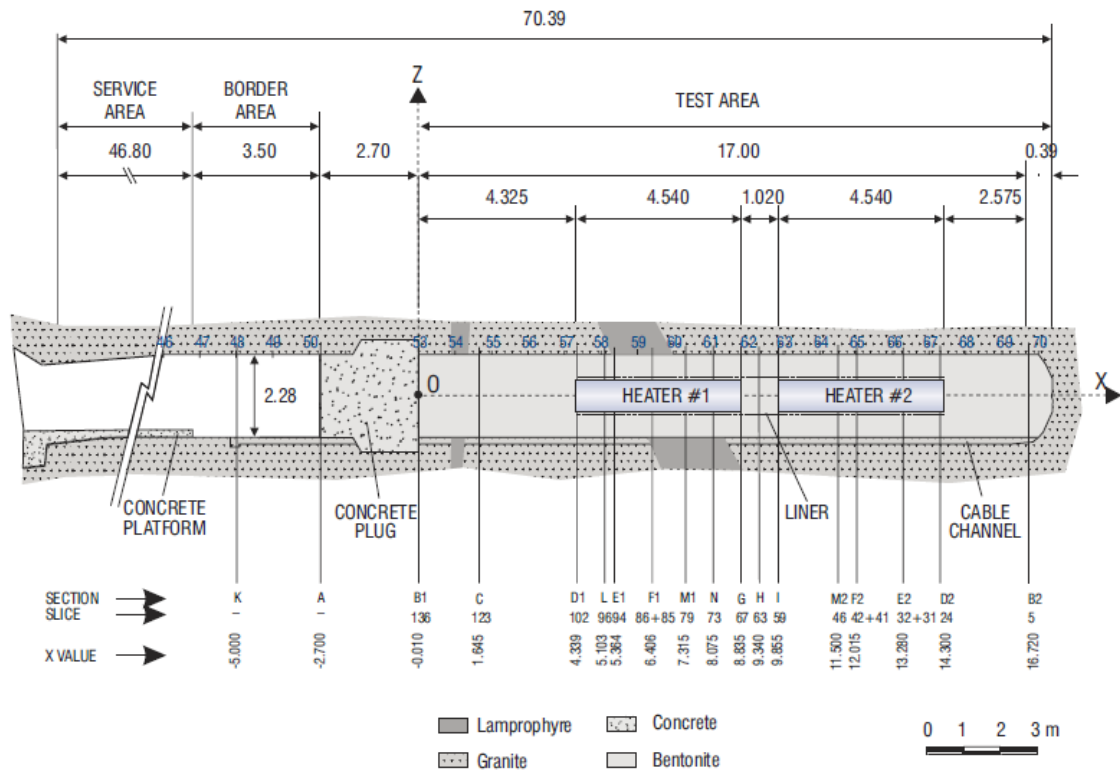


Fig. 2.2: Layout of the FEBEX in situ test, with locations of the sensed sections (from ENRESA, 2006)

2.2 Timeline of the experiment

For the duration of the experiment between 1995 and 2010, it is necessary to distinguish several stages of the experimental setup. After excavation, installation and an initial (isothermal) hydration, a first heating phase maintained the temperature at a constant level of 100 °C. Then, after dismantling of Heater #1, a second heating phase was performed for several years with only Heater #2 in operation. Tab. 2.1 lists dates and durations of the main phases.

Tab. 2.1: Timeline of the FEBEX in-situ test

START	END	Comment	START DAY	END DAY	DURATION [days]
25.09.1995	01.09.1996	Excavation & mechanical Installation (heater 2 finished)	0	342	342
01.09.1996	15.10.1996	Mechanical installation & isothermal hydration of heater 2	342	386	44
15.10.1996	27.02.1997	Isothermal hydration	386	521	135
27.02.1997	28.02.2002	First heating phase	521	2348	1827
28.02.2002	28.05.2002	Cooling phase of heater 1	2348	2437	89
28.05.2002	19.06.2002	Plug demolition	2437	2459	22
19.06.2002	19.07.2002	Heater extraction	2459	2489	30
19.07.2002	29.02.2012	Second heating phase	2489	6001	3512

2.3 Observation data

As mentioned above the FEBEX-site is heavily instrumented site providing measurement data in both, the buffer and the granite rock, from more than 600 sensors for a period of over 15 years. Examples of instrumented sections and positions of the installed sensors area are shown in Fig. 2.3 (longitudinal section), Fig. 2.4 (section F1) and Fig. 2.5 (section F2). For the inverse study at hand only part of the data - a representative set of pressure, temperature and saturation data - have been used from the following boreholes/test sections:

QBF12, cross-section F1: hydraulic pressure in granite (Fig. 2.4)

- Sensor QBF12-01, $r = 12.05$ m
- Sensor QBF12-02, $r = 8.3$ m
- Sensor QBF12-03, $r = 4.53$ m

QBF23: cross-section F2: hydraulic pressure in granite (Fig. 2.5)

- Sensor QBF23-01, $r = 12.68$ m
- Sensor QBF23-02, $r = 9.19$ m
- Sensor QBF23-03, $r = 5.27$ m

QBF24: cross-section F2: hydraulic pressure in granite (Fig. 2.5)

- Sensor QBF24-01, $r = 11.71$ m
- Sensor QBF24-02, $r = 5.22$ m

TBF12, cross-section F1: temperature in granite (Fig. 2.4)

- Sensor TBF12-01, $r = 12.45$ m
- Sensor TBF12-02, $r = 7.59$ m
- Sensor TBF12-03, $r = 2.91$ m

- Sensor TBF12-04, $r = 1.44$ m

TBF23: cross-section F2: temperature in granite (Fig. 2.5)

- Sensor TBF23-01, $r = 10.87$ m
- Sensor TBF23-02, $r = 9.07$ m
- Sensor TBF23-03, $r = 3.03$ m
- Sensor TBF23-04, $r = 1.46$ m

TBF24: cross-section F2: temperature in granite (Fig. 2.5)

- Sensor TBF24-01, $r = 9.11$ m
- Sensor TBF24-02, $r = 2.86$ m
- Sensor TBF24-03, $r = 1.3$ m

TSD1: cross-section D1: temperature, relative humidity in buffer (Fig. 2.6)

- Sensor TSD1-08, $r = 0.81$ m
- Sensor TSD1-10, $r = 1.14$ m

TSD2: cross-section D2: temperature, relative humidity in buffer

- Sensor TSD2-12, $r = 0.81$ m
- Sensor TSD2-13, $r = 1.14$ m

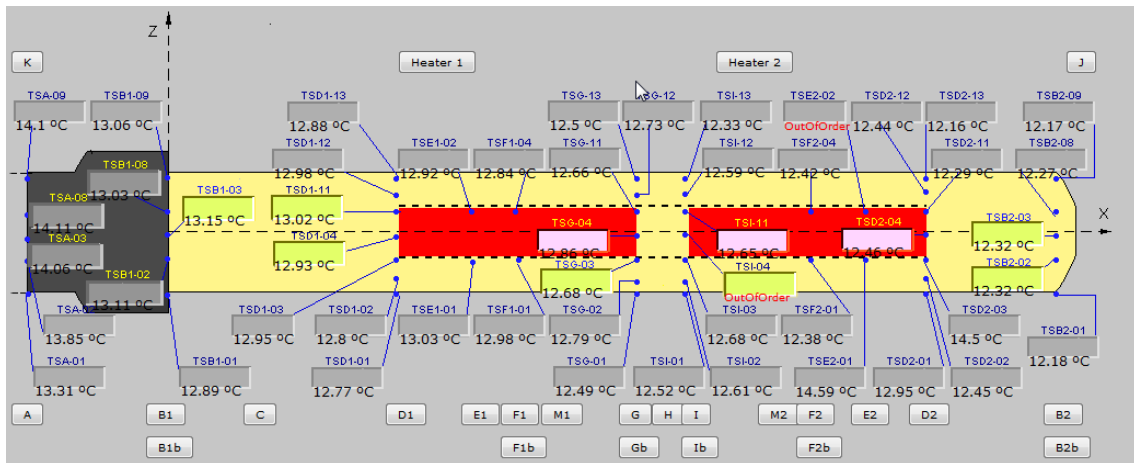


Fig. 2.3: Longitudinal section through test area with location of sensors TSD1-xx (cross-section D1) and TSD2-xx (cross-section D2)

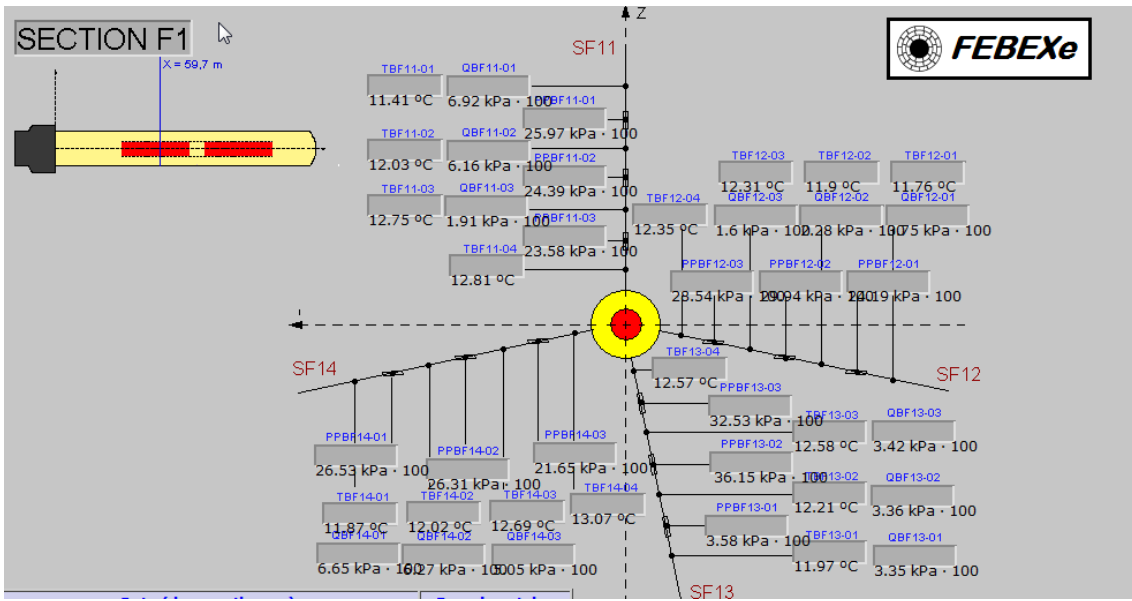


Fig. 2.4: Instrumented section F1 through test area with location of sensors (QBF12-xx, TBF12-xx)

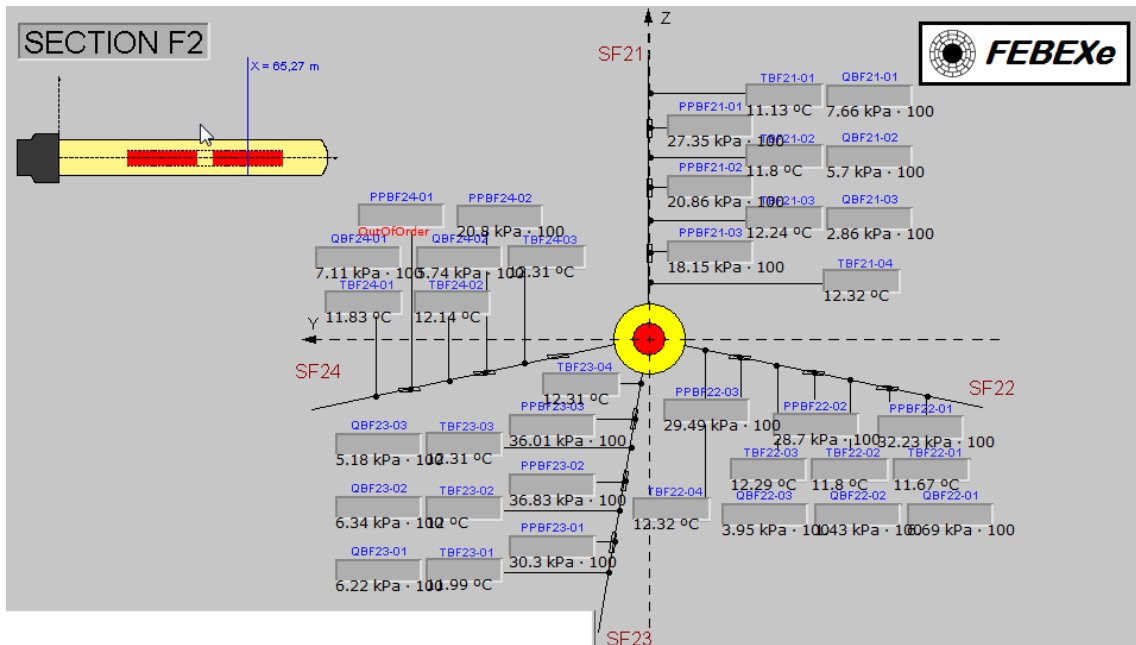


Fig. 2.5: Instrumented section F2 through test area with location of sensors (QBF23-xx, QBF24-xx, TBF23-xx, TBF24-xx)

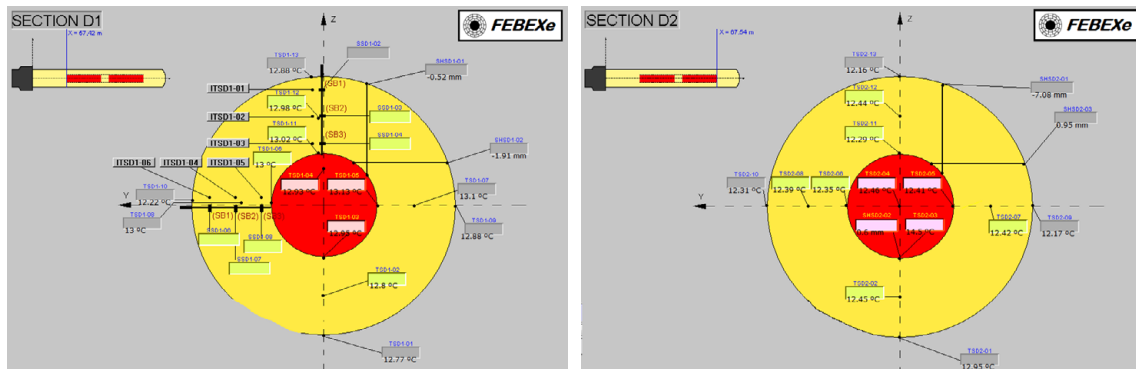


Fig. 2.6: Instrumented section D1 and D2 through test area with location of sensors TSD1-08, TSD1-10, TSD2-12 and TSD2-13

3 Conceptual model

3.1 Modelling approach

It was mentioned in the objectives that, rather than modelling the test by means of a fully coupled Thermo-Hydro-Mechanical code, a computationally more efficient TH approach shall be used to simulate the processes induced by the experiment, namely, resaturation and heat propagation of/in the bentonite buffer and granite host rock. In doing so, mechanical impacts - in particular bentonite swelling - are not considered.

For the computations presented below, the code iTOUGH2 (Finsterle, 2007) is applied, which implements inverse capabilities around the numerical flow simulator TOUGH2 (Pruess et al., 2011). TOUGH2 is capable of dealing with non-isothermal flows of multicomponent, multiphase fluids in one, two, and three-dimensional porous and fractured media. Several equation-of-state (EOS) implementations are available to account for a series of thermo-physical configurations. The present study applies module EOS4 which considers standard non-isothermal two-phase conditions of water and air including vapour pressure lowering effects and the process of vapour diffusion. Regarding details of the inverse framework provided by iTOUGH2 see Chapter 3.5.

Further simplifications introduced for the sake of computational efficiency are the representation of the geometry by an axisymmetric approach (see Chapter 3.2 below) and (as a logical consequence) the neglect of gravity as well as the assumption that the granite rock, buffer and plug material exhibit homogeneous hydraulic and thermal properties.

3.2 Model geometry

As explained in chapter 2 several phases in time of the FEBEX in situ test have to be considered (s. Tab. 2.1). In order to simulate the temporal evolution of the induced flow and heat transport processes in a consistent manner a series of models has to be constructed each representing one phase of the experimental setup, namely, (1) excavation and installation, (2) isothermal hydration, (3) first operational (heating) phase, (4) cooling down of first heater, (5) dismantling of first heater, and (6) second operational phase. The initial conditions being transferred in each case from the previous phase, the 6 models differ in geometry and boundary conditions.

The configurations with their different components associated with the individual experimental phases are implemented by axisymmetric, integrated-finite difference (IFD) meshes according to the TOUGH2 requirements. The different models are listed in Tab. 3.1. Each model corresponds to separate geometrical and/or boundary conditions. Implemented boundary conditions are described in Chapter 3.3. The modelled domain encompassing all components involved along with implemented (hydraulic and heat) boundary conditions are shown in Fig. 3.1. A 3D extension of the axisymmetric mesh for visualization purposes is depicted in Fig. 3.2.

Tab. 3.1: Chain of models with components involved (in addition to open drift entrance and host rock)

Model	Comment	Components
INI	Excavation & mechanical Installation (heater 2 finished)	Test zone empty
ISS	Mechanical installation & isothermal hydration of heater 2	Half of the test zone empty, heater 2 with buffer
ISO	Isothermal hydration	2 heaters, complete buffer, plug
HT1	First heating phase	2 heaters, complete buffer, plug
DMC	Cooling phase of heater 1	2 heaters, complete buffer, plug
DMP	Plug demolition	2 heaters, complete buffer
DMH	Heater extraction	heater 2 with buffer
HT2	Second heating phase	heater 2 with buffer, new plug

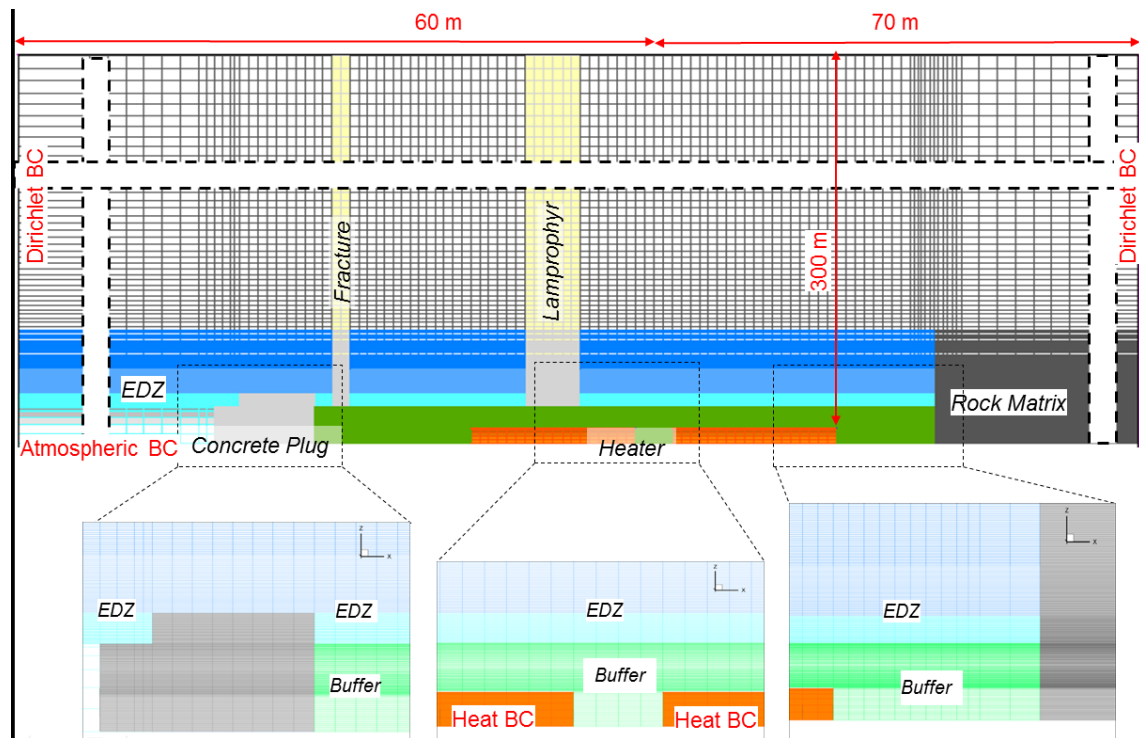


Fig. 3.1: Axisymmetric mesh incl. lamprophyre and fracture FR-2, model dimensions, details and boundary conditions (mesh as used in the heating phase I)

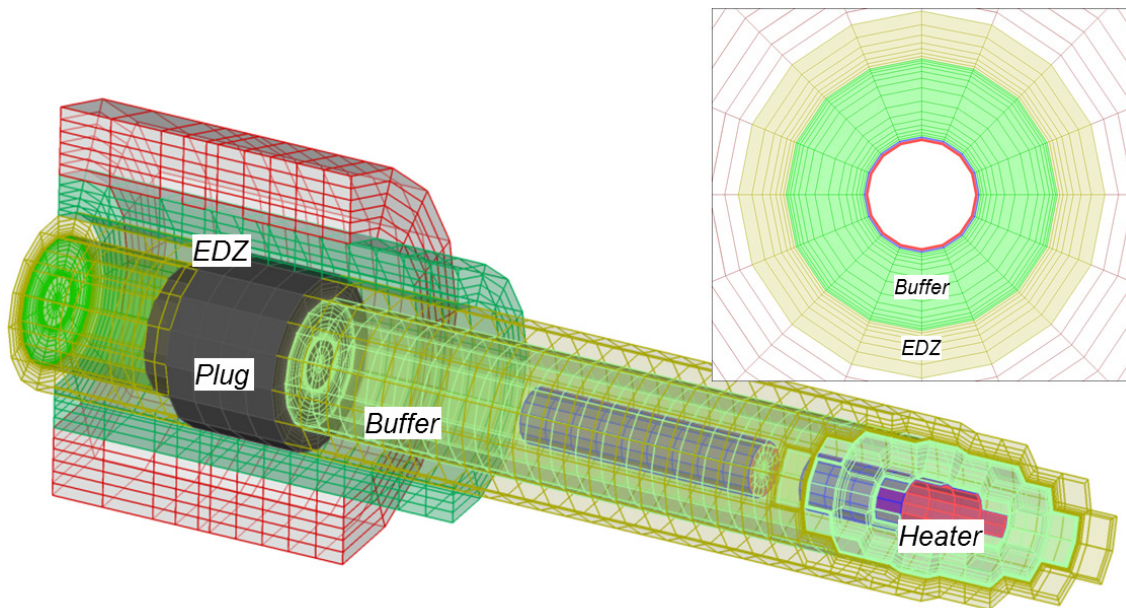


Fig. 3.2: *left*: 3D visualisation of the axisymmetric mesh (Lamprophyre/fracture not shown) *right*: radial mesh refinements at the interfaces between heater, buffer, and EDZ

3.3 Initial and boundary conditions (BC)

3.3.1 Hydraulic conditions

Dirichlet boundary conditions (prescribed pressure) along the lateral boundaries of the model account for the weak natural gradient existing around the FEBEX drift (Fig. 3.3, Fig. 3.1) and represent the basis to compute the initial fully saturated pressure field. In order to simulate the open tunnel, at inner boundaries along tunnel walls as well as at interfaces to the plugs, single phase atmospheric conditions are imposed. Initial saturation of buffer and plugs are given by 55% water saturation.

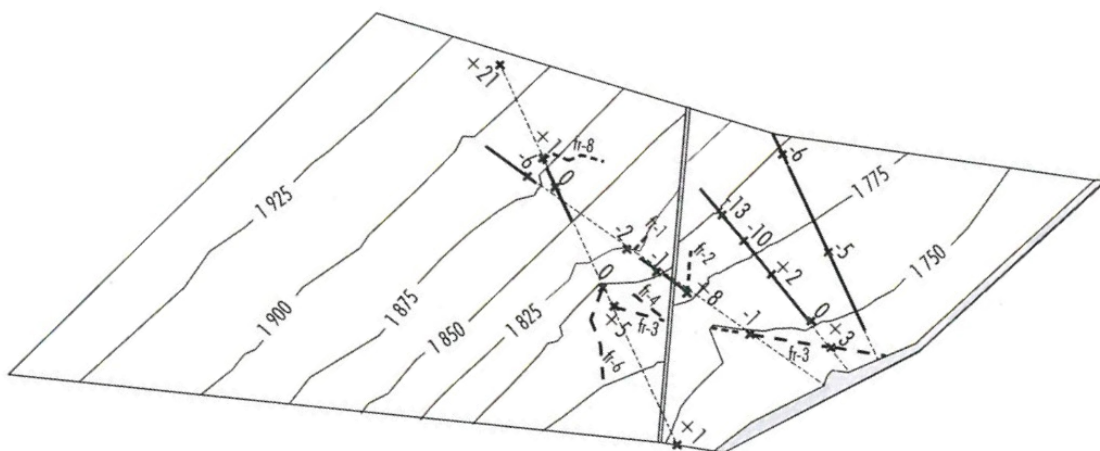


Fig. 3.3: Hydraulic situation in the vicinity of the FEBEX drift, natural flow gradient (from ENRESA, 2006)

3.3.2 Thermal boundary conditions

The initial temperature of the Granite rock as well as the (constant) temperature in the open galleries of the GTS is given by 12 °C (ENRESA, 2006).

The evolution of the heat production realized in the FEBEX as well as the resulting temperature at the boundary of heater 1 is shown in Fig. 3.4. As observed, it could be managed to rise the temperature up to the target of 100 °C within relatively short time and to keep the temperature constant since then for the rest of the measurement period. In the model the two heaters are represented by thin steel liners which obtain an initial temperature according the target of 100 °C. In order to keep the heater temperature constant in the TOUGH2 model a huge heat capacity has been assigned to the liners. In a next phase, cooling of heater 1 is simulated simply by switching the heat capacity to the real value of steel.

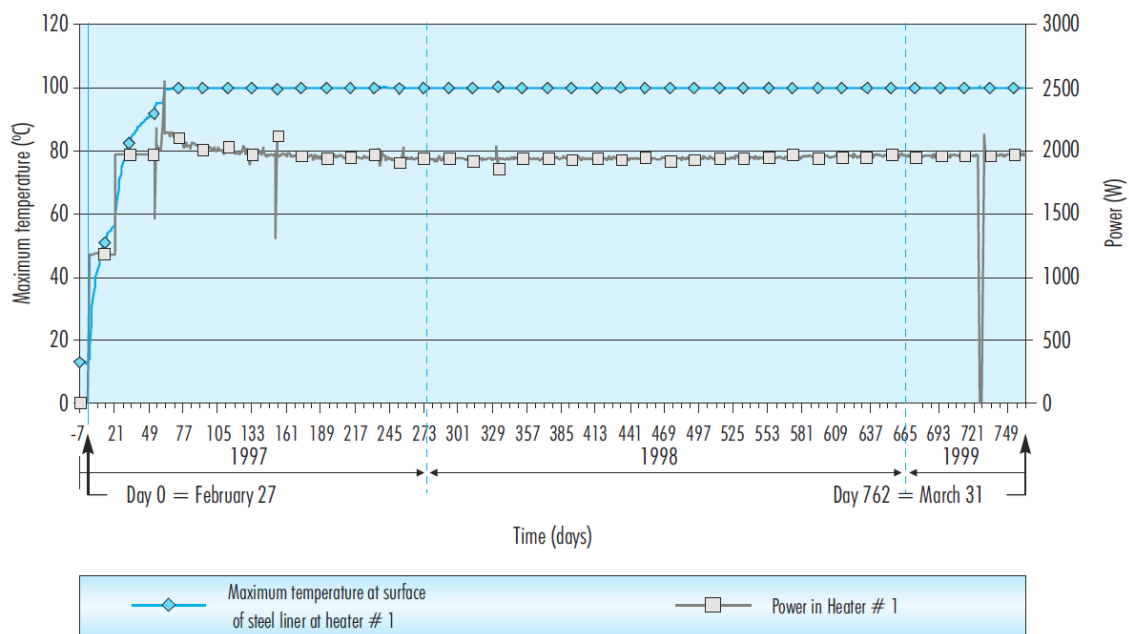


Fig. 3.4: Log of temperature and power in Heater #1 during the first 762 days (from ENRESA, 2006)

3.4 Inverse Framework

In broad terms, inverse modelling refers to the process of gathering information about the model from measurements of what is being modelled. iTOUGH2 is a computer program (Finsterle, 2007) that provides inverse modelling capabilities for the TOUGH2 code. The main purpose of iTOUGH2 is to estimate model-related parameters by automatically calibrating TOUGH2 models to laboratory or field data. In addition, the information obtained by evaluating the sensitivity of the calculated system response with respect to model parameters can also be used to analyse the uncertainty of the parameters and of model predictions.

iTOUGH2 estimates elements of the vector of input parameters based on measured data of the system response. The parameters are related to the data by minimizing a measure of (mis-)fit, the *objective function*, which depends on the residuals between measured and computed system response. In addition, the deviation of estimated parameters from prior information is taken into

account. On certain statistical suppositions, the objective function can be derived from Maximum Likelihood Estimation Theory which finally leads to a weighted least-squares criterion. The iterative procedure of calibration is illustrated in Fig. 3.5. In a first step, an initial guess of parameter values has to be defined. Then, running the model simulates the system response so that residuals with respect to measurements as well as the objective function can be evaluated. After calculation of the Jacobian matrix, which represent the sensitivity coefficients (i.e. derivatives) of measurements with respect to model parameters, an (hopefully) improved set of parameters will be calculated in order to iteratively minimize the objective function.

The inverse approach applied in this study differs from standard applications in that not only one single model has to be run to mimic the experiment for the measurement period of 15 years. Rather, a series of models has to be maintained each representing one phase of the experimental setup, namely, (1) excavation and installation, (2) isothermal hydration, (3) first operational (heating) phase, (4) cooling down of first heater, (5) dismantling of first heater, and (6) second operational phase, as explained above in Chapter 2.2. The initial conditions being transferred in each case from the previous phase, the 6 models differ in geometry and boundary conditions but are driven by the same set of model parameters (Fig. 3.5).

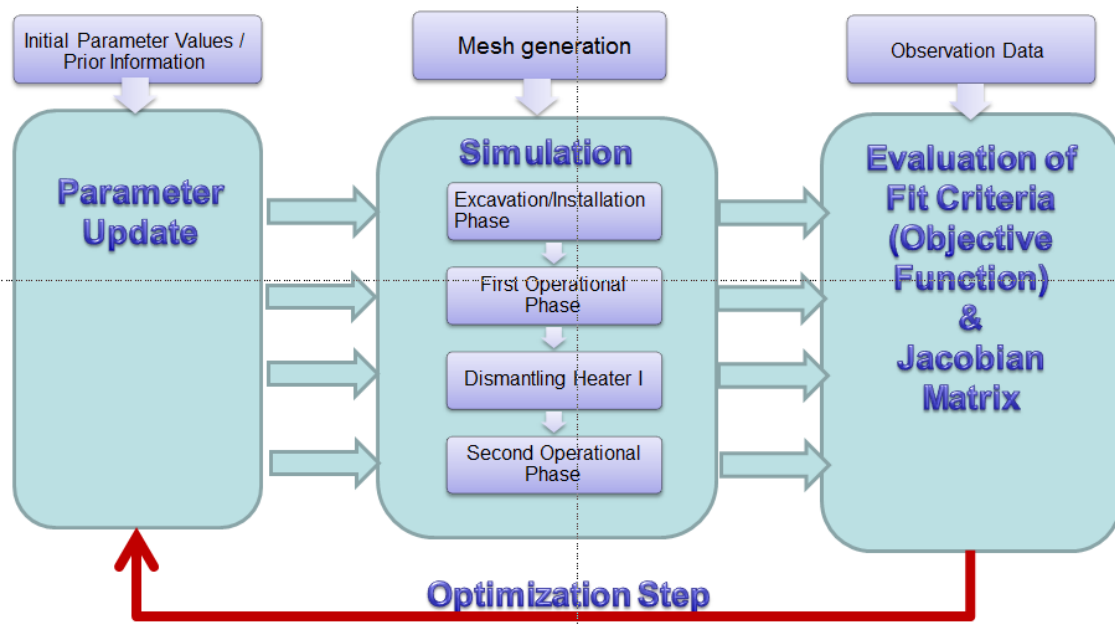


Fig. 3.5: Inverse framework: Iteratively running a series of models in order to minimize the objective function

4 Model parameters, Prior Information

Hydraulic and thermal properties of the Grimsel granite and the FEBEX bentonite have been reported by several authors [Finsterle & Pruess, 1995, Enresa, 2004; ENRESA, 2006; Alonso et al. 2005; Gens et al., 2009). Best guess values used as initial parameters (and prior information in the objective function) are given in Tab. 4.1 for the granite at the GTS and Tab. 4.2 for the FEBEX bentonite. The listed shape parameters of relative permeability and capillary pressure curves, respectively, refer to modified van Genuchten parameter models provided by iTOUGH2 as presented in Tab. 4.3.

Tab. 4.1: Hydraulic and thermal properties of the granite at the Grimsel Test Site (Finsterle & Pruess, 1995; Alonso et al., 2005; ENRESA, 2006)

Property	Prior information	Uncertainty Range	Unit
Density	2660	±23.8	kg/m ³
Porosity	0.01	0.004 - 0.01	-
Absolute Permeability (undisturbed)	1.0E-18		m ²
Absolute Permeability (EDZ)	5.0E-18		m ²
Specific heat	793	750 – 1250	J/kg/°K
Thermal conductivity (wet)	3.34	±0.35	W/m/°K
Thermal conductivity (dry)	2.58	±0.19	W/m/°K
Van Genuchten parameter n	2.5	±0.5	-
Van Genuchten parameter 1/α	1.0	-	MPa
Van Genuchten parameter η	0.5	±0.4	-
Van Genuchten parameter γ	0.333	±0.3	-
Residual liquid saturation	0.01		-

Tab. 4.2: Hydraulic and thermal properties of the FEBEX buffer (Alonso et al.; 2005, ENRESA, 2006)

Property	Prior information	Uncertainty Range	Unit
Density	1600	±23.8	kg/m ³
Porosity	0.4	0.004 - 0.01	-
Absolute Permeability (undisturbed)	1.9E-21		m ²
Specific heat	1091	750 - 1250	J/kg/°K
Thermal conductivity (wet)	1.15	±0.3	W/m/°K
Thermal conductivity (dry)	0.47	±0.2	W/m/°K
Van Genuchten parameter n	2.5	±0.5	-
Van Genuchten parameter 1/α	60.0	-	MPa
Van Genuchten parameter η	0.5	±0.4	-
Van Genuchten parameter γ	0.333	±0.3	-
Residual liquid saturation	0.01		-

Further parameters describing vapour transport in the unsaturated bentonite, such as the vapour diffusion coefficient and tortuosity, parameter values were chosen according to the TOUGH standard input:

- vapour diffusion coefficient: $d_0 = 2.13E-5 \text{ m}^2/\text{s}$
- tortuosity: $\tau_0 = 1$. ($\tau = f(k_{rg})$).

Tab. 4.3: Two-phase (modified) van Genuchten parameter models in iTOUGH2 (Finsterle, 2012) used for all materials

capillary pressure

relative permeability

$P_c = P_o \cdot (S_{ec}^{n/(1-n)} - 1)^{1/n}$ $S_{ec} = \frac{S_l - S_{lr}}{1 - S_{lr}}$ $m = 1 - 1/n$	$k_{r,l} = S_e^\eta \cdot \left[1 - (1 - S_e^{1/m})^m \right]^2$ $k_{rg} = (1 - S_{ekg})^\zeta \left[1 - S_{ekg}^{1/m} \right]^{2m}$ $S_e = \frac{S_l - S_{lr}}{1 - S_{gr} - S_{lr}}$ $S_{ekg} = \frac{S_l}{1 - S_{gr}}$
---	--

5 Results

5.1 Simulations results

The current chapter describes simulation results based on the final set of model parameters. Simulated pressure distributions are illustrated in Fig. 5.1. The pressure cone observed after the excavation phase (INI), partially (phase ISO) and almost fully recovers during the first heating phase (HT1). Temperature distributions are shown in Fig. 5.2. The heat front is moving into the granite for a distance of approximately 10m from the axis during the first heating phase. Cooling and only 1 heater operating reduces the radius of influence to 7 m, approximately.

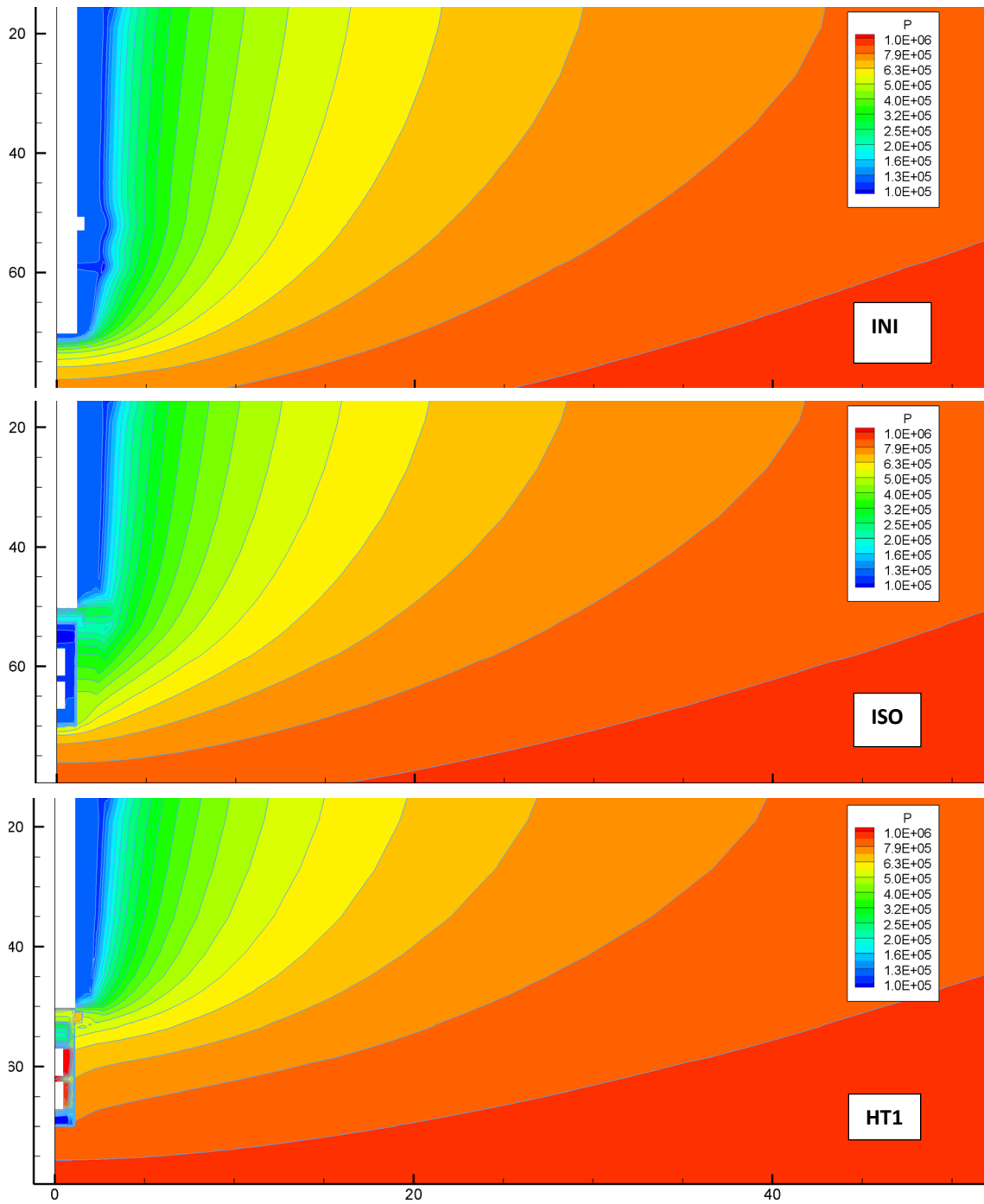


Fig. 5.1: Pressure distribution after excavation (phase INI), isothermal hydration (ISO), operational phase I (HT1)

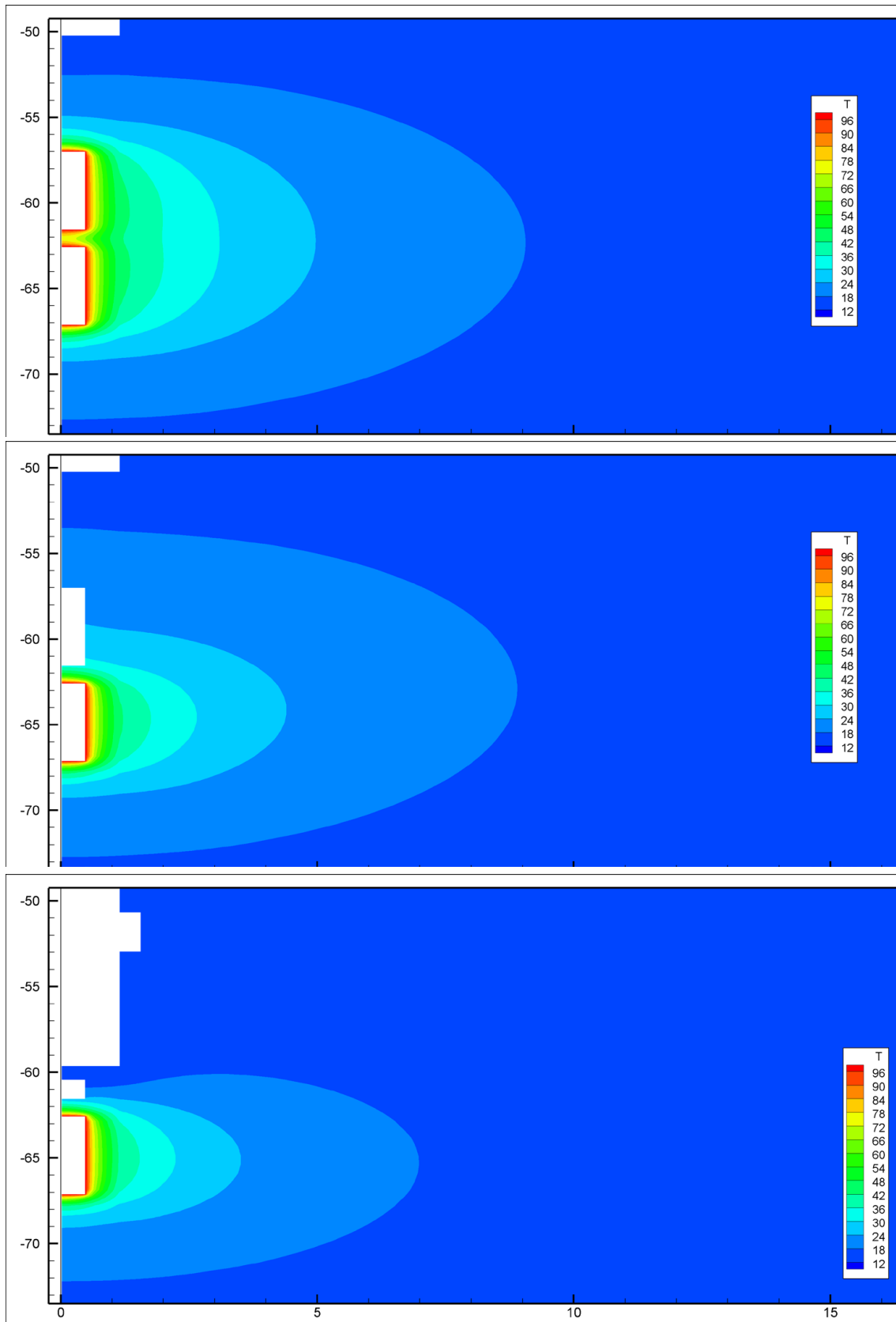


Fig. 5.2: Temperature distribution after heating phase 1 (HT1), cooling down of Heater#1 (phase DMC), and after second heating phase with only heater#2 operating (HT2)

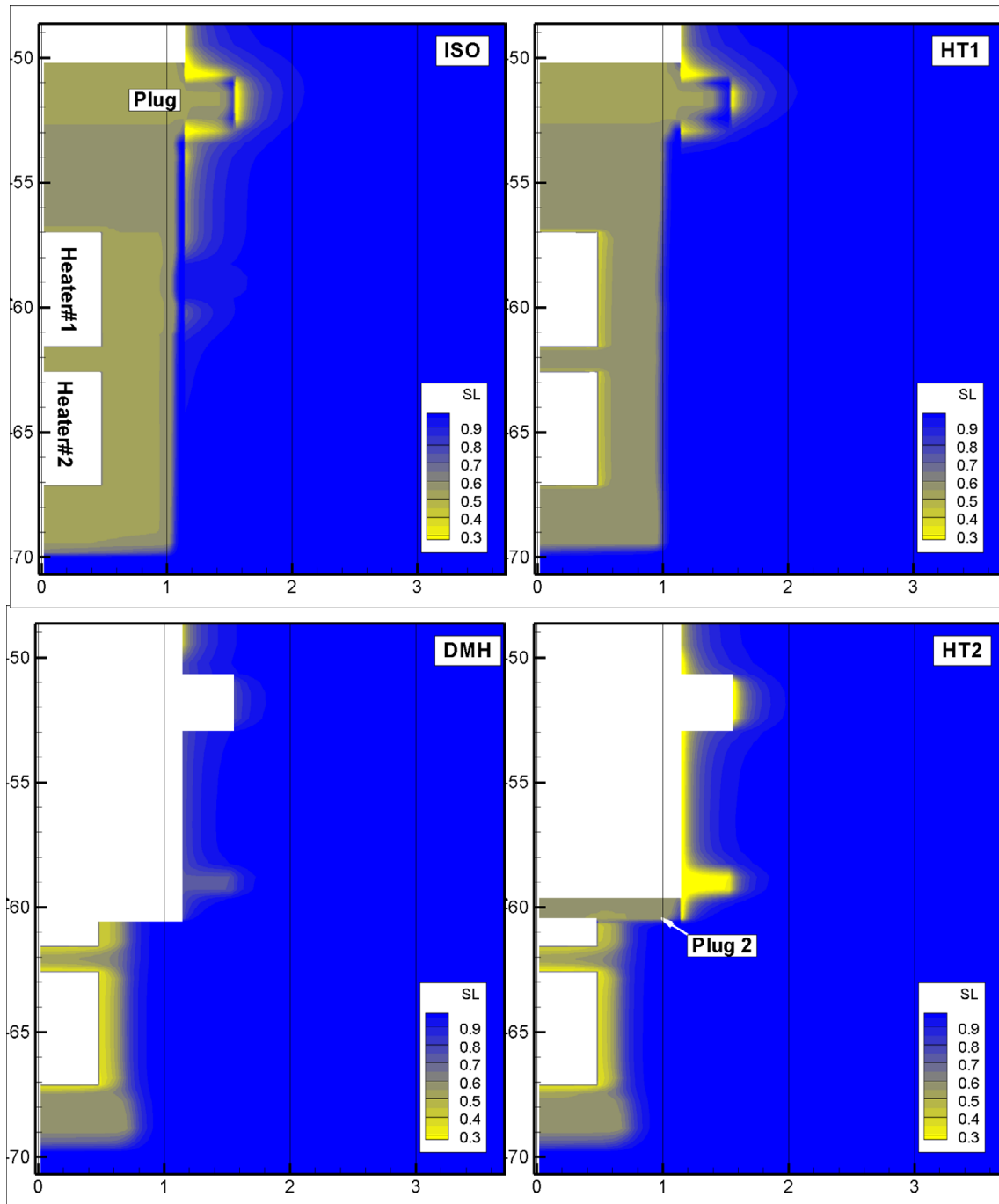


Fig. 5.3: Distribution of water saturation after isothermal hydration (phase ISO), heating phase 1 (HT1), dismantling of Heater#1 (DMH), heating phase 2 (HT2)

5.2 Residual analysis

5.2.1 Pressure

Evolution of pressure as measured in granite is displayed in Fig. 5.4 and Fig. 5.5 and compared to computed counterpart. As observed (e.g. from sensors QBF11 and QBF14, which have

approximately the same distance from the heaters), the measurements exhibit strong differences in dependence of the borehole direction (s. Fig. 2.4, Fig. 2.5). Presumably, this is an effect of host rock heterogeneity and/or a (vertical) pressure gradient. Although the measurements have been corrected for the (small) static component with respect to the axis, this behaviour (by definition) cannot be reproduced by means of the present axisymmetric approach. Also measurement errors seem to be present. While the pressure drop after dismantling of Heater#1 is observed in most of the sensors and reproduced quite well by the model in some of them (e.g. QBF11-03, QBF12, etc.) measurements in sensors QBF24 do not show any drop although recovery during heating phase 1 agrees quite well with the simulations.

5.2.2 Temperature

In contradiction to pressure results simulated temperatures show amazing agreement with experimental observations (Fig. 5.6 to Fig. 5.9). In most of the sensors, mean absolute residuals between model and measurement are less than 1°C in both, the granite and the bentonite. The disagreement in Section G after dismantling (Fig. 5.9) probably points to poor modelling of the new concrete plug closing heater#2 from the open drift. Further comparisons are attached in the Appendix.

5.2.3 Relative humidity

Comparison of measured and modelled relative humidity (RH) is shown in Fig. 5.10 for sensors installed in the bentonite of section F1 and F2. While the sensors observe some heterogeneity in RH depending on their azimuths the axisymmetric model confirms a good representation of the measured average. However, the model fails to reproduce the dry-out observed at low radius in the centre between the two heaters in Section H (Fig. 5.11).

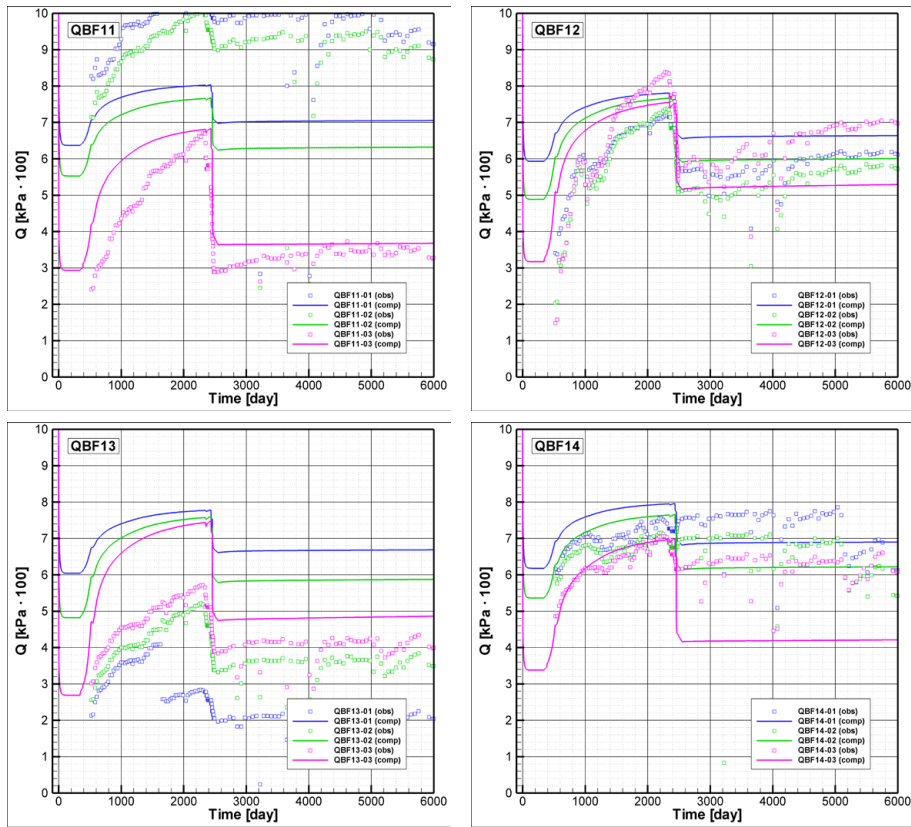


Fig. 5.4: Cross section F1 - comparison of measured and computed pressure in granite

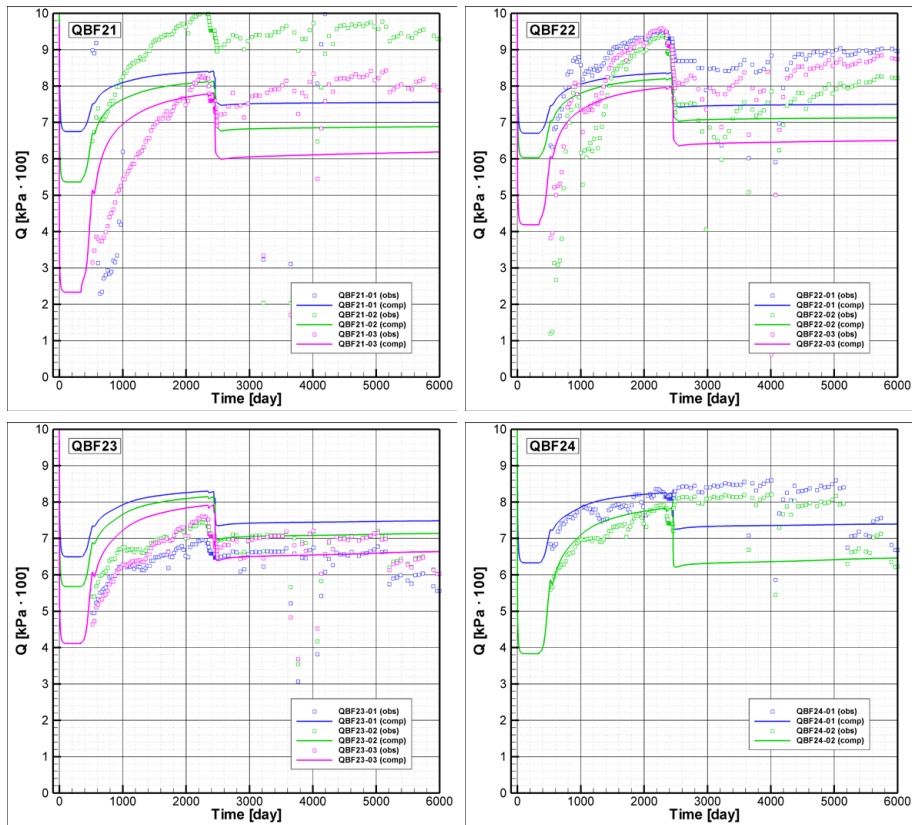


Fig. 5.5: Cross section F2 - comparison of measured and computed pressure in granite

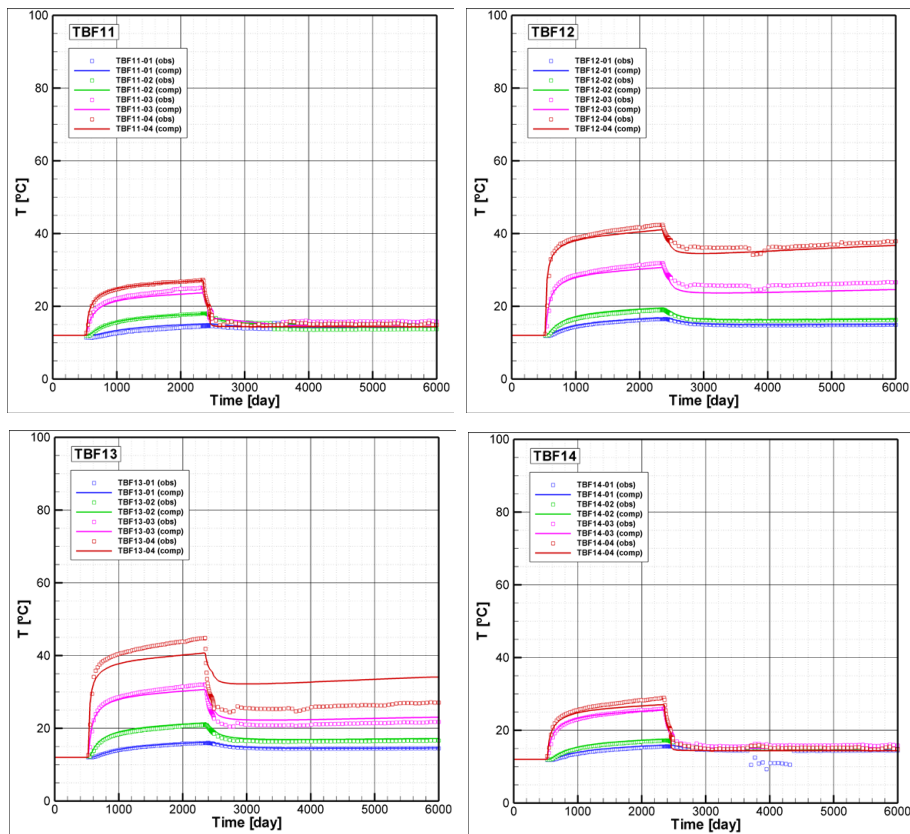


Fig. 5.6: Cross section F2 - comparison of measured and computed temperature in granite

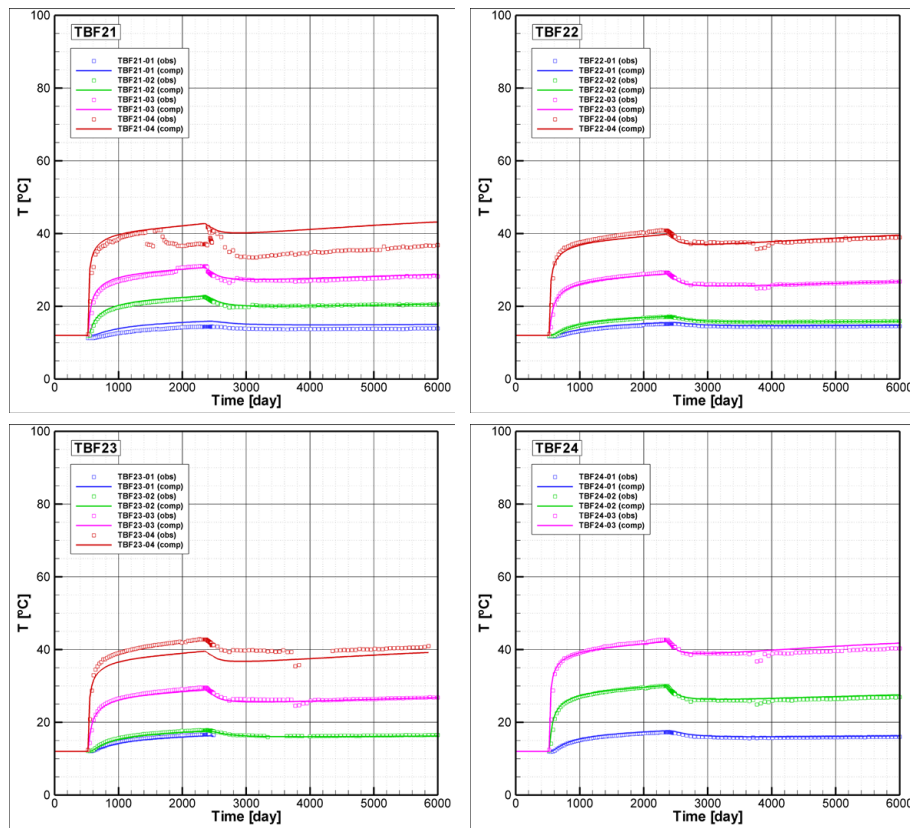


Fig. 5.7: Cross section F2 - comparison of measured and computed temperature in granite

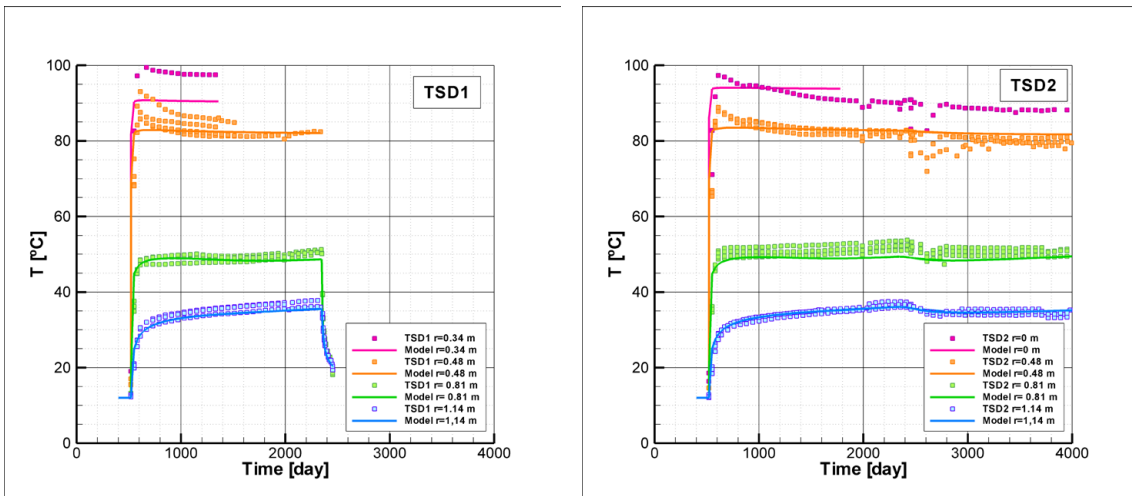


Fig. 5.8: Cross sections D1 (left) and D2 (right) - comparison of measured and computed temperature in bentonite (locations see Fig. 2.3)

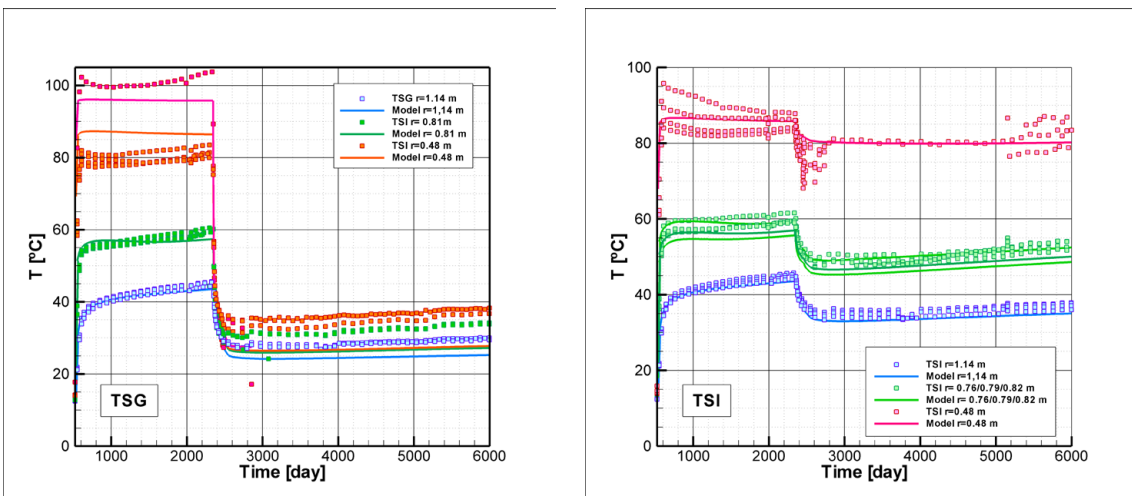


Fig. 5.9: Cross sections G (left) and I (right) - comparison of measured and computed temperature in bentonite (locations see Fig. 2.3)

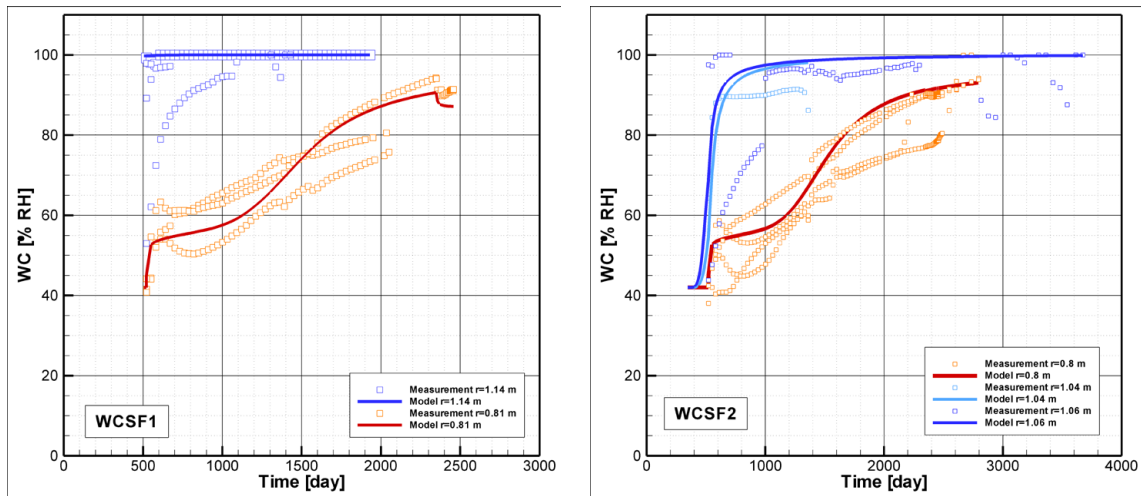


Fig. 5.10: Cross sections F1 and F2 - comparison of measured and computed relative humidity in bentonite

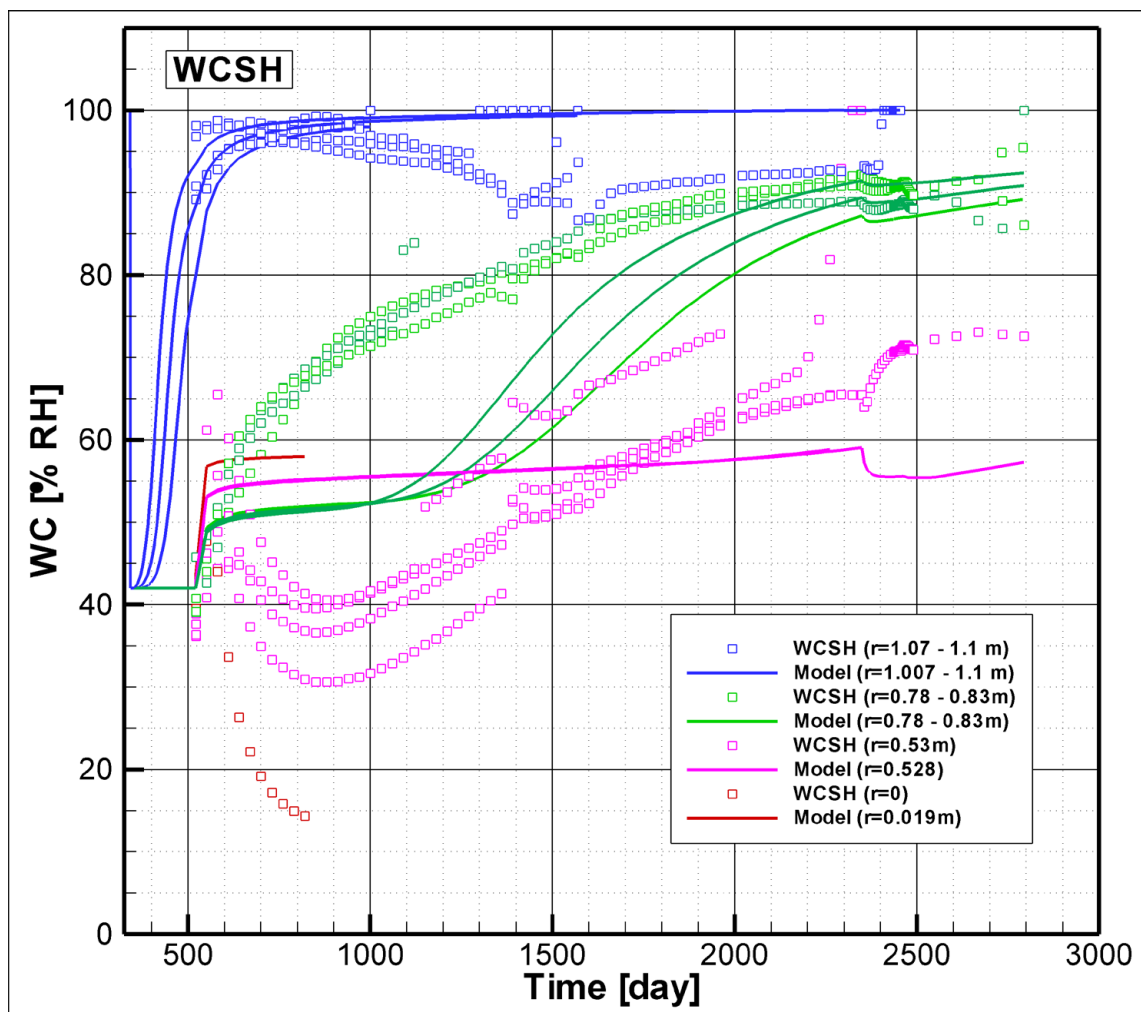


Fig. 5.11: Cross section H - comparison of measured and computed relative humidity in bentonite

5.3 Estimated parameters

The joint inversion of the whole set of measurement data results in parameter estimates of permeability, porosity, relative permeability and capillary pressure functions for both, host rock and bentonite buffer. The final parameter values are listed in Tab. 5.1. The applied retention curves provided by a modified version of the van Genuchten model (see Finsterle, 2012) of both, the Grimsel granite and the FEBEX bentonite are illustrated in Fig. 5.12. Exponential law and parameters of the thermal conductivity model are shown in Fig. 5.13. The resulting curves fit quite well into the available laboratory measurements.

In addition to parameter estimates the inverse study provides error estimates in form of covariance and correlation matrices, confidence intervals as well as standard deviations. The latter are indicated in brackets in Tab. 5.1.

Following comments on the model parameters should be considered:

- Porosity of FEBEX bentonite.

The porosity of about 6% resulting from inverse modeling of the FEBEX-in-situ experiment seems to be very low compared to about 40 % measured in laboratory tests. However, the estimated value is a best fit parameter which is able to reproduce the relative humidity measurements in the buffer reasonably well. It is understood, that this value represents a mean (TH-model) parameter reflecting the simplifications made by neglecting mechanical impacts such as bentonite swelling, etc.

- Two-phase parameters of granite.

The estimated air entry pressure of ~ 0.6 MPa seems to be low compared to measurements and prior modeling studies (Finsterle & Pruess, 1995). Because in the inverse model (FEBEX-in-situ) both, intact host rock and EDZ have the same two-phase model parameters this value probably refers rather to the inner zone of the EDZ where micro-fractures may lead to reduced capillary pressure.

- Permeability of EDZ

It is surprising, that the estimation of EDZ-permeability is lower than the estimation of undisturbed rock. This result has to be interpreted in conjunction with the computation of the hydraulic conductivity in the (mostly unsaturated) EDZ where the product of absolute and relative permeability is one term. It is probable, that in the unsaturated EDZ a (non-unique) combination of relative and absolute permeability computes the reduced conductivity while in the saturated undisturbed rock relative permeability does not have any impact. Usually, such behaviour can be circumvented by appropriate weighting of the prior information.

Tab. 5.1: Hydraulic, thermal and two-phase properties of the different materials resulting from inverse modelling of the FEBEX-in-situ experiment (in brackets the computed standard deviations)

	Unit	Granite	EDZ	FEBEX-Bentonite
Density	ρ [kg/m ³]	2630	2630	1735
Specific Heat	C_r [Jkg ⁻¹ K ⁻¹]	910	910	1170
Thermal Conductivity (Eq. 1) - Dry - Wet	T_k [Wm ⁻¹ K ⁻¹]	3.63(0.16) 3.44(0.87)	3.63(0.16) 3.44(0.87)	1.22(0.06) 0.48(0.03)
Thermal Expansion	T_x [K ⁻¹]	-	-	$1.5 \cdot 10^{-5}$
Initial Water Saturation	S_w [-]	1.0	1.0	0.66
Porosity	ϕ [-]	0.012(0.0004)	0.033(0.004)	0.055(0.005)
Permeability	k [m ²]	$6.8 \cdot 10^{-19}(0.02)^*$	$4.4 \cdot 10^{-19}(0.03)^*$	$9.4 \cdot 10^{-22}(0.03)^*$
Pore Compressibility	C_p [Pa ⁻¹]	$2 \cdot 10^{-11}$	$2 \cdot 10^{-11}$	$2 \cdot 10^{-9}$
Van Genuchten parameters (s.)				
- n	[-]	2.34(0.12)	2.34(0.12)	1.42(0.02)
- $1/\alpha$	[Pa]	$0.6 \cdot 10^{-6}(0.03)^*$	$0.6 \cdot 10^{-6}(0.03)^*$	$2.96 \cdot 10^{-7}(0.01)^*$
- η	[-]	0.5(0.01)	0.5(0.01)	0.5(0.05)
- ζ	[-]	0.02(0.003)	0.02(0.003)	0.4(0.05)
Residual Water Saturation	S_{irk} [-] S_{irc} [-]	0.01 0.01	0.01 0.01	0.01 0.01
Residual Gas Saturation	S_{gr} [-]	0	0	0
Vapour Diffusion Coefficient	[m ² /s]			

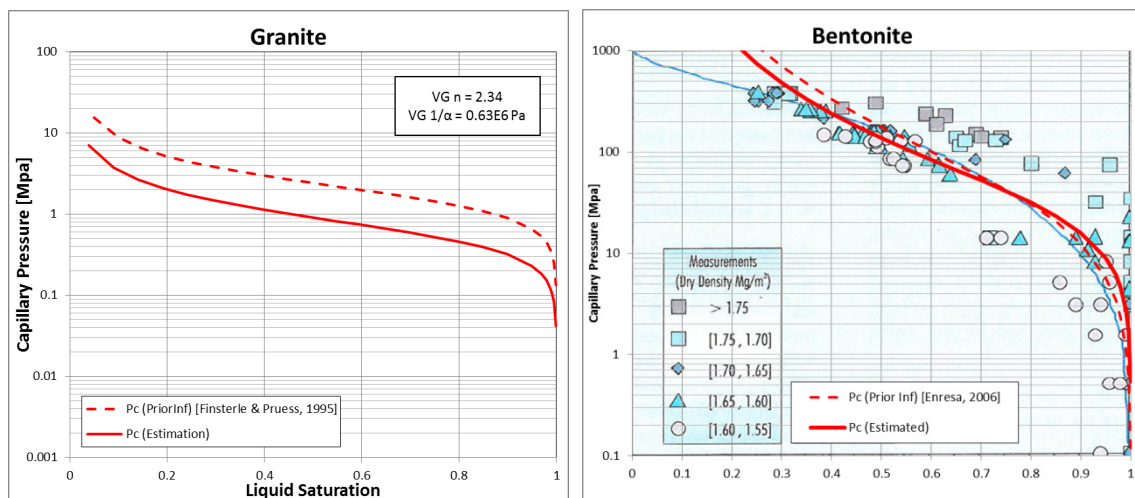


Fig. 5.12: Retention curves of Grimsel granite and FEBEX bentonite (adapted from ENRESA, 2006)

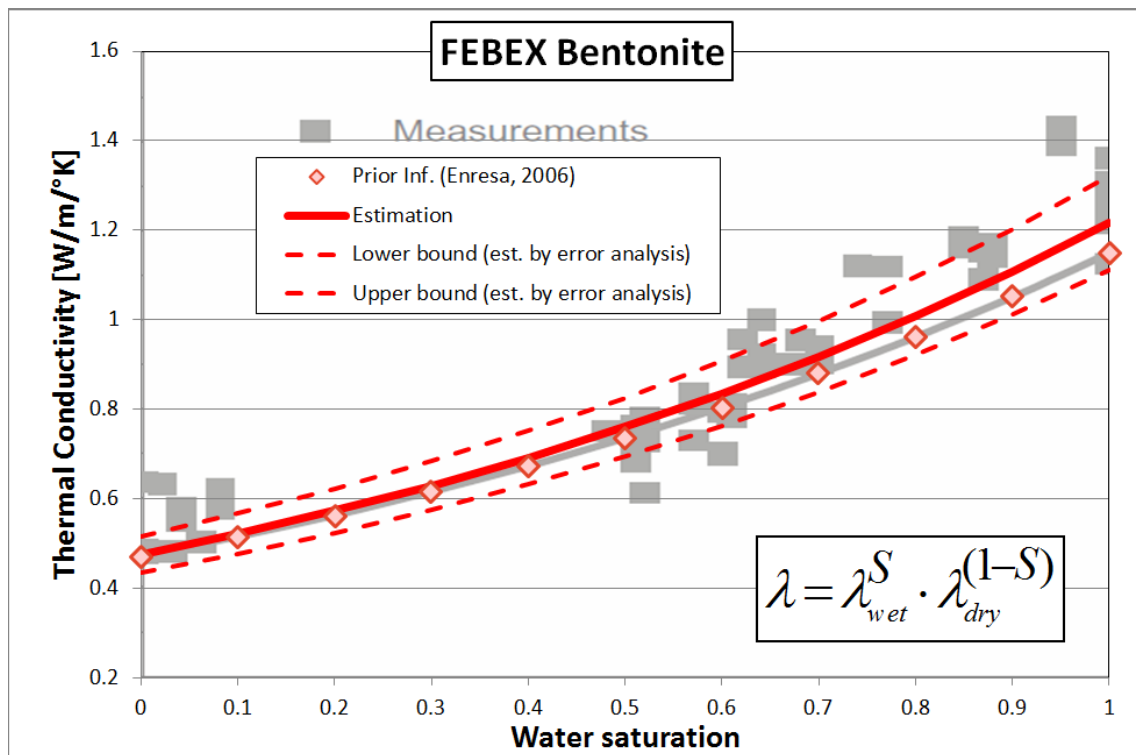


Fig. 5.13: Thermal conductivity and error range of FEBEX bentonite estimated by inverse modelling (adapted from ENRESA, 2006)

6 Summary and Conclusion

This study was motivated by PEBS Task WP 3.3 and studied if TH inverse approaches can be applied for interpreting long term THM experiments as well as PEBS Task WP 3.5 which has to deal with extrapolation of findings from the (relatively short term) experimental and modelling efforts of the PEBS project. In this context, the long term evolution of heat as emitted by nuclear waste on the saturation behavior of the engineered barrier system (EBS) has to be simulated. Rather than applying the coupled thermo-hydro-mechanical approach (THM) it would be computationally more efficient to use a TH-code (such as iTOUGH2), thus, neglecting mechanical processes as induced e.g. by bentonite swelling. In order to ensure predictive reliability, the present study derives the involved model parameters from inverse modelling of the full-scale FEBEX in-situ test which provides pressure, temperature, and saturation data from a heating experiment for a period of 15 years.

The inverse approach applied in this study differs from standard applications in that not only one single model can be run to simulate the experiment for the measurement period of 15 years. Rather, a series of models has to be maintained each representing one phase of the experimental setup, which includes, (1) excavation and installation, (2) isothermal hydration, (3) first operational (heating) phase, (4) cooling down of first heater, (5) dismantling of first heater, and (6) second operational phase. The initial conditions being transferred in each case from the previous phase, the 6 models differ in geometry and boundary conditions but are driven by the same set of model parameters.

The joint inversion of the whole set of measurement data results in parameter estimates of permeability, porosity, relative permeability and capillary pressure functions for both, host rock and bentonite buffer. Comparisons of model simulations with the observations show different agreement. While the pressure fit obtained in the granite boreholes is suffering from the unconsidered heterogeneity and potential measurement errors the agreement of relative humidity in the buffer and temperature in both, buffer and rock is amazing taking into account the simplicity of the axisymmetric model. Moreover, the estimated thermal and two-phase parameter values fit well into the range of available laboratory measurements. Other parameter estimates (e.g. the low porosity of the bentonite) include the influence of then neglected/simplified processes and, thus, refer to the TH modelling approach, solely.

In addition, the inverse model provides uncertainty estimates of the resulting parameters in form of standard deviations which can be applied in following modelling steps in order to assess the uncertainty of long term predictions. Moreover, this type of modelling contributes to the understanding of the early behaviour of the EBS system until full saturation is reached and the assessment of the impact of processes (such as chemical processes) which depend on the saturation state and its evolution in time.

Further conclusions are:

- It is common understanding that inverse modelling helps minimizing the bias of the modeller. However, some bias remains because observations of diverse origin as well as prior information have to be weighted subjectively defining the objective function. In this context, e.g. the question arises: what would have happened if the heads in the granite (which have only poor agreement) had been excluded from the analysis?
- As the FEBEX is located in a very rigid granitic hostrock environment, neglecting the mechanical aspects might be more acceptable than would have been the case in a more plastic clay type host rock type such as the Opalinus Clay. In a follow up step, based on the

experience gained with inverse modelling in this study, the methodology will be applied to the 1:2 scale HE:E heater test in Mont Terri.

- Interesting future developments would be to apply the methodology to establish an optimized hydraulic conductivity versus saturation relationship as well as a porosity versus saturation relation for the bentonite (again to mimic the impact of the swelling and reduction in permeability and porosity)

7 References

- Pruess, K., C. Oldenburg, G. Moridis (2011), TOUGH2 User's Guide, Version 2, Lawrence Berkeley National Laboratory, LBNL-43134 (revised), 2011
- Enresa (2001), ENRESA-2000, Granite Repository Performance Assessment.
- Enresa (2006), FEBEX – Full-scale Engineered Barriers Experiment, Updated Final Report 1994-2004, publicación técnica 05-2/2006.
- Finsterle, S. (2007), iTOUGH2 User's Guide, LBNL-40040 Revised, Earth Sciences Division, Lawrence Berkeley National Laboratory, University of California, Berkeley, California, February 2007.
- Finsterle, S. (2012), iTOUGH2 Command Reference, LBNL-40041 Revised, Earth Sciences Division, Lawrence Berkeley National Laboratory, University of California, Berkeley, California, March 2012.
- Gens A, Sánchez M, Guimarães LDN, Alonso EE, Lloret A, Olivella S, Villar MV (2009), A full-scale in situ heating test for high-level nuclear waste disposal: observations, analysis and interpretation. *Geotechnique* 2009; 59(4):377–399.
- Martinez-Landa, L., and Carrera J., 2006. A methodology to interpret cross-hole tests in a granite block. *Journal of Hydrology* Volume 325, (1-4, 30) (June), pp.222-240.
- PEBS (2010) Long-term performance of engineered barrier systems, Description of work, Seventh Framework Programme, European comission, 2010
- Pruess, K., C. Oldenburg, G. Moridis (2011), TOUGH2 User's Guide, Version 2, LBNL-43134 (revised), Earth Sciences Division, Lawrence Berkeley National Laboratory, University of California, Berkeley, California, August 2011.

8 Appendix

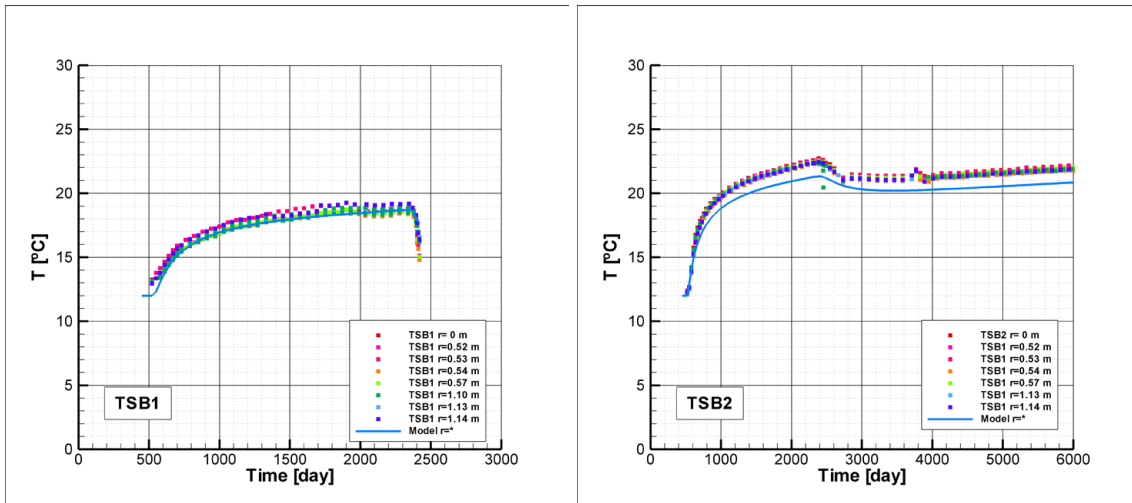


Fig. A.1: Temperature – Section B1, B2

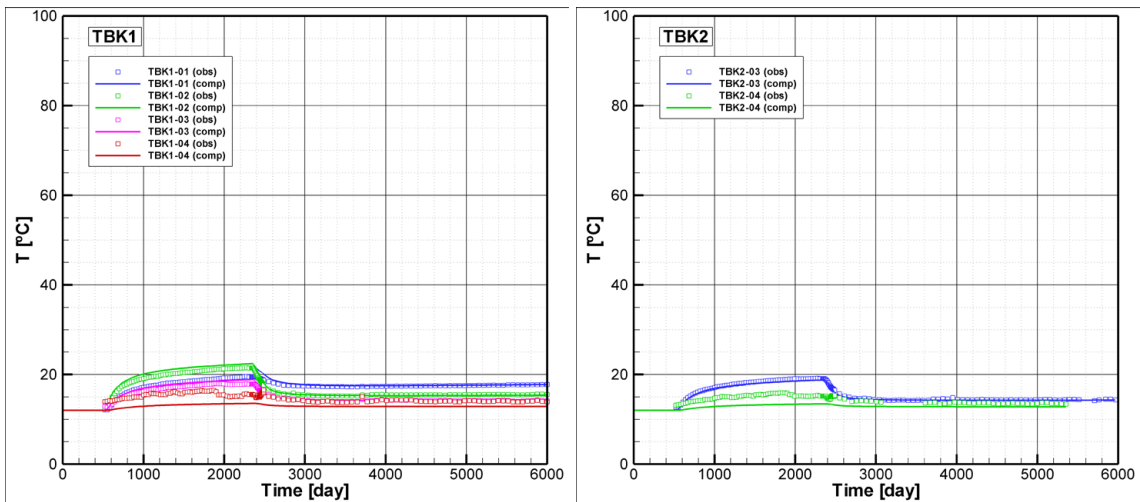


Fig. A.2: Temperature – Section K1, K2